DOI: 10.1002/ejic.201100212

Optimization of the Efficiency of Oxidation Catalysts Based on Iron Bispidine Complexes

Peter Comba,*[a] Hubert Wadepohl,[a] and Sebastian Wiesner[a]

Keywords: Homogeneous catalysis / Oxidation / Iron / Bioinspired catalysis / Rigid ligands

High-valent bispidine iron-oxo complexes are among the most efficient nonheme iron oxidation catalysts. Here, we report the synthesis and structural analysis of two derivatives of the known pentadentate bispidine ligand L^1 {L^1 = 2,4-pyridyl-7-(pyridine-2-ylmethyl)-3,7-diazabicyclo[3.3.1]nonane}: L^2 and L^3 {L^2 = 2,4-pyridyl-7-[1-(pyridine-2-yl)ethyl]-3,7-diazabicyclo[3.3.1]nonane; L^3 = 2,4-pyridyl-7-[phenyl(pyridine-2-yl)methyl]-3,7-diazabicyclo[3.3.1]nonane}, and of their Fe^{II} complexes. The yield of the catalytic epoxidation of cyclooctene and styrene with iodosylbenzene as oxidant increases from the L^1- to the L^2- to the L^3-based catalyst (e.g., the yield of styrene oxide, with MeCN as solvent, under anaerobic conditions, is 40 %, 90 %, 96 %, respectively), and this is correlated to the $Fe^{III/II}$ reduction potentials {$[Fe(L^1)(NCMe)]^{n+}$ (1.01 V), $[Fe(L^2)(NCMe)]^{n+}$ (1.13 V), and $[Fe(L^3)(NCMe)]^{n+}$ (1.19 V), in MeCN, vs. SCE}. Although this correlation is not unexpected, the interpretation is not entirely trivial, and this is discussed in detail. The rigidity of the bispidine ligands and their preference for relatively large metal ions (low oxidation states, high spin multiplicities) is believed to be responsible for the efficiency of the bispidine-based catalyst systems, and the present results show possible approaches to further improve the performance of these catalysts.

Introduction

The oxidation of olefins is an important reaction in organic synthesis, and epoxidation catalyzed by transition metal complexes is a promising approach for the efficient preparation of a variety of building blocks for subsequent transformations.[1] Biomimetic manganese,[2–4] as well as heme- and nonheme iron catalysts[5–7] have been developed, studied in detail with respect to reaction mechanism and scope, and have been shown to include efficient, selective, and economically as well as environmentally viable systems.

Due to the availability of a wide variety of easy to prepare tetra- and pentadentate bispidine ligands (2,4- and 3- or 7-substituted 3,7-diazabicyclo[3.3.1]nonane; see Scheme 1 for the pentadentate 2,4,7-substituted bispidines L^1–L^3 discussed in this communication) and based on their rich coordination chemistry,[8] their oxygen activation performance with copper,[9–12] cobalt,[13] vanadium,[14] ruthenium,[15,16] and iron[17–21] systems have been studied in detail. The iron systems in particular have been shown to be efficient oxygenation catalysts, and the iron chemistry of the L^1-based pentadentate as well as the corresponding 2,4-substituted tetradentate bispidine ligands have indeed been shown to have, among the corresponding families of iron complexes, the highest $Fe^{IV/III}$ reduction potentials and the highest efficiencies in a range of C–H activation and oxygen-transfer reactions.[19–23] One of the main reasons for the high redox potentials and interesting electronic properties (e.g., a relatively low ligand field) is the extremely rigid bispidine backbone with a well preorganized and relatively large cavity, and, therefore, with a preference for higher spin multiplicities and lower oxidation states.[24–28] In a qualitative sense, this indicates that the $Fe^{IV/III}$ and the $Fe^{III/II}$ potentials are correlated, and this is of importance and will be discussed in more detail below.

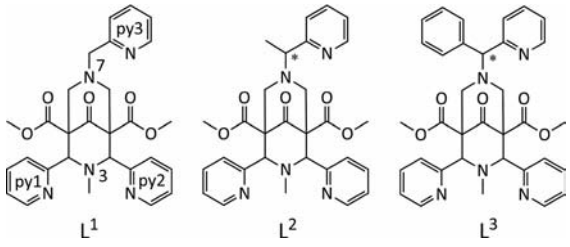

Scheme 1. Pentadentate bispidine ligands.

An attractive idea to support this interpretation and to use it as a concept to increase the redox potentials and therefore also to improve the performance of these catalysts, was to further increase the rigidity of the pentadentate bispidine ligands. Since the five-membered chelate ring involving the picolylamine-derived substituent py3 of L^1 is the only flexible part of the corresponding complexes (see Scheme 1), the obvious idea was to block this conformational flexibility. Five-membered chelate rings of this type may be reinforced by substituents at the α-position to the amine, and this approach yielded the methyl-substituted ligand L^2 and the phenyl-substituted ligand L^3. Both L^2 and

[a] Universität Heidelberg, Anorganisch-Chemisches Institut, Im Neuenheimer Feld 270, 69120 Heidelberg, Germany
Fax: +49-6221-546617
E-mail: peter.comba@aci.uni-heidelberg.de

L^3 have been prepared to study their iron oxidation chemistry. The optically pure forms of L^2 and L^3 have also been isolated, but the enantioselectivity of the catalytic oxidation processes with the corresponding Fe^{II} complexes is, due to the remote site and the relatively small perturbation of the high symmetry, as expected, very low, and this will not be discussed in the present communication.

Results and Discussion

Syntheses, Structural Properties, and $Fe^{III/II}$ Reduction Potentials

Ligands L^2 and L^3 were prepared in good yields in analogy to L^1[29] but by using the corresponding substituted picolylamine-derived building blocks,[30–32] and the corresponding iron complexes were obtained in analogy to those of L^1.[33] Racemic samples were used for structural and electrochemical experiments as well as for the epoxidation reactions. Compounds used for optical rotation spectroscopy were obtained from ligands prepared with the enantiomerically pure amine precursors. With the exception of [Fe(*R*-L^2)(Cl)]Cl, the samples for crystallographic analyses were from racemic compounds. Shown in Figure 1 are plots of the X-ray crystal structure analyses of L^2 and L^3 as well as of the corresponding (chlorido)iron(II) complexes. Due to the high solubility and slow crystallization of L^2, the crystallographic sample for L^2 was prepared as the picric acid adduct. The structures of the metal-free ligands show the expected geometries of the bispidine cavity with a chair-boat conformation of the fused six-membered rings for L^3, and, due to double protonation and therefore reduced lone-pair–lone-pair repulsion, the chair-chair conformation for H_2L^{2+}.[8] The three structures of the molecular cations of the Fe^{II} complexes of L^1–L^3 are very similar, and, as expected, from other bispidine-based Fe^{II} complexes,[8,33] with distances of the tertiary amine, pyridine, and halide donors to the high-spin Fe^{II} center in the expected ranges (see Table 1 and Figure 1).[34]

Pathways for the catalytic oxidation of organic substrates, mediated by nonheme iron complexes, generally involve ferryl complexes, and their reactivity must be correlated to a large extent to the redox potentials (oxidation power) of the high-valent iron-oxo complexes,[35,36] that is, the driving force is the main parameter of interest. There are a number of recent reports on the relevant $Fe^{IV/III}$=O reduction potentials, and there are at least three conceptually different methods, not all of which are unambiguous and free of some controversy.[35–39] So far, there is no published comparative study, and some work along these lines is presently being done with the compounds reported here and other bispidine complexes of iron. Here, we report and discuss the pertinent $Fe^{III/II}$ redox potentials in relation to the structural properties and catalytic efficiencies. We believe that, for the very rigid bispidine ligands with identical donor sets (L^1–L^3), the size, shape, and elasticity of the ligand cavities are the major and decisive variables that are responsible for the relative stabilities of the oxidation

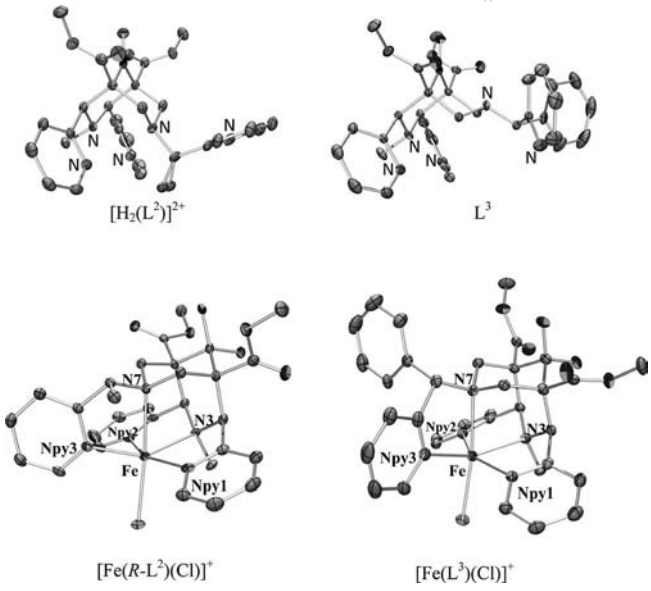

Figure 1. ORTEP plots of the ligands $[H_2(L^2)]^{2+}$ (crystallized as picrate; only one of the sites of the disordered Me group is shown) and L^3 (top), and of the molecular cations (bottom) of [Fe(*R*-L^2)(Cl)]$^+$ and [Fe(L^3)(Cl)]$^+$ (ellipsoids are drawn at the 50% probability level, hydrogen atoms and counterions are omitted for clarity).

Table 1. Structural parameters of the high-spin iron(II) complexes of three differently substituted bispidine ligands (distances in Å, angles in °).

	$[Fe^{II}(L^1)(Cl)]^+$[33]	$[Fe^{II}(R\text{-}L^2)(Cl)]^+$	$[Fe^{II}(L^3)(Cl)]^+$
Fe–N3	2.194(2)	2.204(2)	2.213(2)
Fe–N7	2.362(2)	2.379(2)	2.342(2)
Fe–Npy1	2.182(2)	2.223(2)	2.173(2)
Fe–Npy2	2.142(2)	2.148(2)	2.232(2)
Fe–Npy3	2.134(2)	2.138(2)	2.143(2)
Fe–X	2.416(1)	2.3767(7)	2.3616(7)
Npy1···Npy2	4.195(2)	4.244(3)	4.265(3)
N3···N7	2.879(2)	2.881(3)	2.938(3)
N3–Fe–N7	78.27(5)	77.81(7)	80.29(7)
N3–Fe–Npy3	152.59(7)	149.25(7)	153.70(8)
N7–Fe–X	170.64(7)	171.12(5)	171.96(5)
Npy1–Fe–Npy2	151.82(6)	152.25(8)	151.05(8)

states,[40] and this should independently be the case for the $Fe^{III/II}$ and the $Fe^{IV/III}$ potentials. Note that we are fully aware that the yield of an oxidation reaction (the turnover number of a catalytic oxidation process) is not necessarily expected to be correlated to the driving force of the process (i.e. the redox potential), and this will need some further exploration.[41]

The L^1-based Fe^{IV}=O system is known to be one of the most efficient nonheme iron oxidation catalysts with a pentadentate ligand system,[17,20,21] and this was found to be correlated to the redox potential and to be due to a large extent to the rigidity and specific size and shape of the bispidine cavity.[23,25,26] It was therefore expected that the sterically reinforced ligands L^2 and L^3, where the chelate ring involving py3, the only flexible part in the coordinated ligand system, is enforced to a specific conformation, have

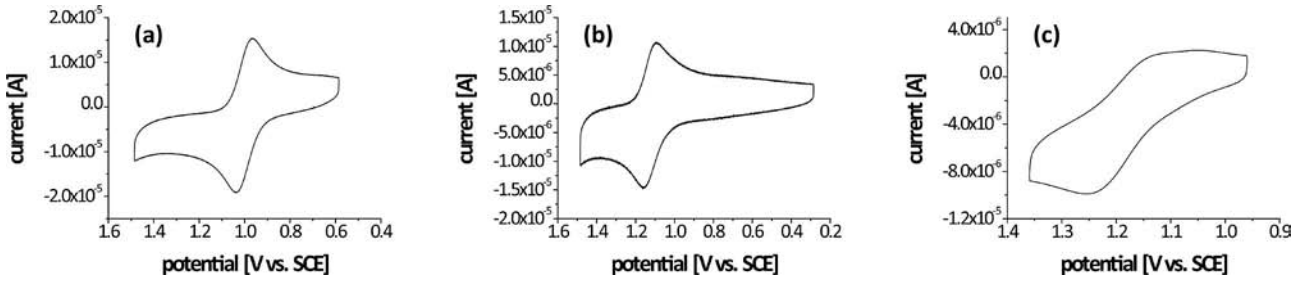

Figure 2. Cyclic voltammograms of the $Fe^{3+/2+}$ couples of the complex cations in MeCN (0.1 M Bu_4NClO_4) of (a) ligand L^1 (1.00 V, ΔE = 70 mV), (b) ligand L^2 (1.12 V, ΔE = 74 mV), L^3 (1.18 V, ΔE = 141 mV; note that this CV is not clean, for unknown reasons, with a second possible wave at ca. 1.15 V, ΔE = 203 mV).

Table 2. Redox potentials of the precatalysts {$[Fe(L^n)(NCMe)]^{3+/2+}$ (n = 1,2,3)} and product distribution of the catalytic oxidation of styrene and cyclooctene with $[Fe(L^n)(NCMe)]^{2+}$ (n = 1,2,3) and PhIO as oxidant (MeCN, 25 °C).[a]

Catalyst	$Fe^{III/II}$ potential [V] vs. SCE	Styrene → benzaldehyde + styrene oxide TON: max = 100		Cyclooctene → cyclooctene oxide TON: max = 100	
$[Fe(L^1)(NCMe)]^{2+}$	1.00	11.9	40.5	4.2	
$[Fe(L^2)(NCMe)]^{2+}$	1.12	2.5	90.2	10.2	
$[Fe(L^3)(NCMe)]^{2+}$	1.18	1.7	95.5	8.5	

[a] All measurements are based on the dry triflates (OTf = $CF_3SO_3^-$) of the high-spin Fe^{II} complexes (fast ligand exchange) in MeCN, i.e., MeCN is assumed to be the coligand.

an even more restricted elasticity and therefore lead to an increasing destabilization of the high-valent form and consequently to more efficient oxidants. The $Fe^{III/II}$ reduction potentials with the three ligands with increasing rigidity (in MeCN, vs. SCE, see Figure 2 and Table 2) confirm this expectation, that is, the $Fe^{III/II}$ potentials increase in the series $[Fe(L^1)(NCMe)]^{n+}$ (1.00 V, Δ = 70 mV), $[Fe(L^2)(NCMe)]^{n+}$ (1.12 V, Δ = 74 mV), $[Fe(L^3)(NCMe)]^{n+}$ (1.18 V, Δ = 141 mV).

Epoxidation Catalysis

The (bispidine)iron-catalyzed epoxidation of cyclooctene with L^1 was studied in detail under aerobic and anaerobic conditions, by using various solvents and oxidants (MeCN, H_2O, MeOH; H_2O_2, tBuOOH, PhIO) and, in combination with ^{18}O labeling studies ($H_2{}^{18}O$, $H_2{}^{18}O_2$, $^{18}O_2$), spectroscopy, and computational work, a mechanism involving Fe^{IV}=O and a carbon-based radical intermediate was established.[17,18,28,42] The L^1-based iron oxidation catalyst is one of the most efficient nonheme iron systems and indeed has the highest $Fe^{IV/III}$ redox potential (H^+-coupled electron transfer) measured so far and, more importantly, the potentials of the H^+-coupled electron transfer of a group of nonheme iron catalysts have been shown to be correlated to the efficiencies of C–H activation and oxygen-transfer processes.[23] Here, we report the corresponding reactivities of the structurally reinforced L^2- and L^3-based iron catalysts (see Scheme 2).[41] Reported in Table 2 are the catalytic activities of the three systems with iodosylbenzene (PhIO) as the oxidant, under anaerobic conditions and in MeCN as solvent, with a catalyst loading of 1 mol-% and a maximum turnover number (TON) of 100, with styrene and cyclooctene as the substrates.

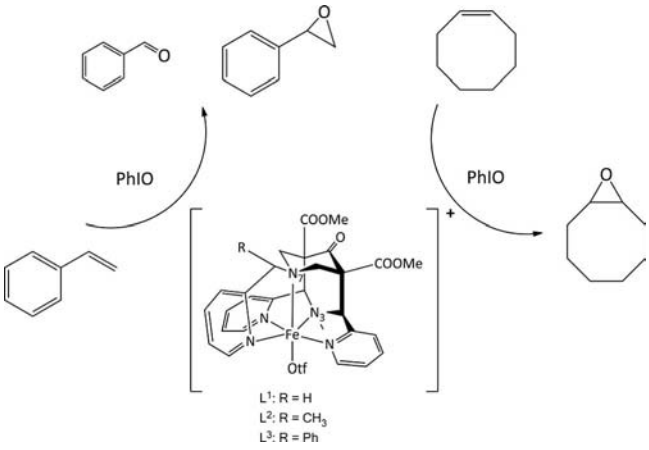

Scheme 2. Oxidation reactions studied with Fe^{II} precatalysts based on L^1, L^2, and L^3.

The yield is generally higher for styrene oxidation than for cyclooctene oxidation, but the trend for the three catalysts is similar for the two substrates. The increasing yield is correlated to the $Fe^{III/II}$ redox potentials of the three catalysts:[43] with styrene in MeCN there is an increase from approx. 50% to 90% and a nearly quantitative yield of oxidation products, with epoxide to aldehyde ratios of 3.5, 36, and 56.

Conclusions

We have shown that a simple substitution of the pentadentate bispidine ligand L^1 leads to a substantial increase of the redox potential of the corresponding iron complexes ($Fe^{III/II}$ couples; due to the rigidity of the bispidine backbone, this is presumably also true for the $Fe^{IV/III}$ couples)

and a concomitant increase in the catalytic activity towards olefin oxidation. We interpret these observations as follows: (i) Redox potentials of transition metal complexes are strongly influenced by steric effects, and these may be enforced by the ligand backbone; with a constant couple [$Fe^{III/II}$ (or rather $Fe^{IV/III}$ in terms of the catalytically active species) in our series], a constant solvent (MeCN) and a constant ligand sphere (three pyridines and two tertiary amines of the pentadentate bispidines), the size and shape of the ligand cavity is the only (or at least the major) variable. (ii) Bispidine ligands (specifically also pentadentate ligands of the type L^1–L^3) have rather large and very rigid cavities; this leads to a stabilization of the lower oxidation states, that is, to relatively high redox potentials. (iii) An active oxidation catalyst needs to have a high redox potential, that is, an unstable oxidized form of the catalyst. Related to (ii), it appears that the only flexible part of the pentadentate bispidine L^1, that is, the pendant pyridine py3 (see Scheme 1) may help to somewhat stabilize the high-valent iron complex and therefore, a reduction of the flexibility might lead to even more powerful oxidants – the results in Table 2 seem to confirm this idea.

Experimental Section

General Remarks: Chemicals (Aldrich, Fluka) and solvents were of the highest possible grade and they were used as purchased. The bispidine ligand L^1 and its Fe^{II} complex were prepared as described before.[33] Elemental analyses were performed by the analytical laboratories of the chemical institutes of the University of Heidelberg. Electronic spectra were measured with a Tidas II J&M or a Jasco V-570 UV/Vis/NIR spectrophotometer. For electrochemical measurements, a BAS-100B workstation was used, with a three-electrode setup, consisting of a glassy carbon working, a Pt-wire auxiliary, and an $Ag/AgNO_3$ reference electrode [$AgNO_3$ (0.01 M), Bu_4NPF_6 (0.1 M), in degassed MeCN]. The complexes were dissolved in MeCN/Bu_4NClO_4 (0.1 M); the potential of the Fc^+/Fc-couple had a value of +95 mV (380 mV vs. SCE, MeCN, scan rate of 200 mV s^{-1}). NMR spectra were recorded at 200.13 MHz (^1H) and 50.33 MHz (^{13}C) with a Bruker AS-200 or a Bruker DRX-200 instrument with the solvent signals as reference. IR spectra were recorded with a Perkin–Elmer Spectrum 100 FT-IR spectrometer instrument from KBr pellets. Mass spectra were obtained with a JEOL JMS-700 or Finnigan TSQ 700/Bruker ApexQe hybrid 9.4 FT-ICR instrument. For optical rotations a Jasco DIP 370 polarimeter and for CD spectra a Jasco J 710 spectropolarimeter were used.

X-ray Crystal Structure Determinations: Crystal data and details of the structure determinations are listed in Table 3. Intensity data were collected at low temperature [100(2) K] with a Bruker AXS Smart 1000 CCD diffractometer (Mo-K_α radiation, graphite monochromator, λ = 0.71073 Å). Data were corrected for air and detector absorption, Lorentz and polarization effects;[44] absorption by the crystal was treated with a semiempirical multiscan method.[45,46] The structures were solved by conventional direct methods[47,48] (L^3), by the heavy atom method combined with structure expansion by direct methods applied to difference structure factors[49] {complexes [Fe(*R*-L^2)(Cl)]Cl and [Fe(L^3)(Cl)]Cl}, or by direct methods with dual-space recycling ("Shake-and-Bake")[50] (L^2), and refined by full-matrix least-squares methods based on F^2 against all unique reflections.[48,51] All non-hydrogen atoms were given anisotropic displacement parameters. Hydrogen atoms were generally input at calculated positions and refined with a riding model. In the structures of free ligands L^2 and L^3, the positions of most hydrogen atoms (except those of the methyl groups) were taken from difference Fourier syntheses and refined. The structure of the protonated racemic L^2 was refined in $P\bar{1}$. However, the distribution of the two enantiomers among the two symmetry equivalent sites in the unit cell is not equal, resulting in a disorder of the methyl group C26A/C26B on the asymmetric carbon center [refined occupancies 0.697(5):0.303(5)]. The hydrogen atoms resulting from protonation of L^2 by picric acid were located on N3 (bispidine backbone) and N4 (py3). Additional electron density was typically found in the structures of the complexes, some of which could be assigned to discrete solvent molecules {disordered water and acetonitrile in [Fe(L^2)(Cl)]Cl and water and ethanol in [Fe(L^3)(Cl)]Cl}. Still unassigned electron density in the latter structure (possibly disordered ethanol) was removed from the structure (and the corresponding F_{obs}) with the BYPASS procedure,[52] as implemented in PLATON (SQUEEZE).[53] Crystallographic data (excluding structure factors) for the structures reported in this paper have been deposited with the Cambridge Crystallographic Data Center: CCDC-751130 (L^2), -751131 (L^3), -751132 [(L^2)Fe(Cl)]Cl, and -751133 [(L^3)Fe(Cl)]Cl. These data can be obtained free of charge via www.ccdc.cam.ac.uk/data_request/cif.

L^2: A sample of 1-methyl-4-oxo-2,6-bis(2-pyridyl)piperidine-3,5-dicarboxylic acid dimethyl ester (3.0 g, 7.8 mmol) was suspended in methanol (50 mL) and cooled to 0 °C. At this temperature, (*S*)-1-(pyridinyl-2yl)ethylamine (1.1 g, 9 mmol) was added dropwise, and the mixture was stirred for 30 min. Then formaldehyde (1.3 mL, 16 mmol, 37% in water) was added. After being stirred for 24 h at room temperature, the mixture was concentrated to dryness. Recrystallization from 2-propanol gave crystalline L^2; yield 2.1 g (3.9 mmol, 50%). The racemic as well as the (*R*)-configured compound were synthesized in the same manner as stated above. Optical rotation (S): $[\alpha]_D^{20}$ = –18.6 (c = 2, in $CHCl_3$); (*R*): $[\alpha]_D^{20}$ = 18.0 (c = 2, in $CHCl_3$). $C_{29}H_{31}N_5O_5$ (529.23): calcd. C 65.77, H 5.90, N 13.22; found C 65.89, H 5.92, N 13.16. FAB-MS: calcd. for [L^2 + H]$^+$ 529.6; found 530.4. ^1H NMR (200 MHz, $CDCl_3$): δ = 1.35 (d, ^3J = 6.9 Hz, 3 H, CH-CH_3), 1.93 (s, 1 H, N-CH_3), 2.63 (dd, ^4J = 5.7, ^2J = 11.9 Hz, 2 H, CH_{eq}-CH_{ax}), 3.13 (d, ^2J = 11.9 Hz, 2 H, CH_{ax}-CH_{eq}), 3.70 (s, 3 H, O-CH_3), 3.72 (s, 3 H, O-CH_3), 4.61 (s, 2 H, N-C*H*), 7.05–8.05 (m, 9 H, H_{Ar}), 8.40 (dd, ^4J = 0.6, ^3J = 4.7 Hz; 2 H, H_{Ar}), 8.51 (d, ^3J = 4.8 Hz, 1 H, H_{Ar}) ppm. ^{13}C NMR (50 MHz, $CDCl_3$): δ = 16.28 (CH-*C*H_3), 43.63 (N-*C*H_3), 52.79 (*C*H-CH_3), 55.67/56.37 (N-*C*H_2-C_q), 62.80/62.98 (C_q), 65.31 (O-*C*H_3), 74.10/74.23 (N-*C*H-Py), 122.74, 123.29, 123.94, 124.49, 136.62, 149.53, 158.77, 159.01, 160.59 (C_{Ar}); 169.14 (-*C*OOCH_3), 204.04 (*C*=O) ppm.

L^3: A sample of 1-methyl-4-oxo-2,6-bis(2-pyridyl)piperidine-3,5-dicarboxylic acid dimethyl ester (1.056 g, 2.7 mmol) was suspended in methanol (15 mL) and cooled to 0 °C. At this temperature, (*S*)-phenyl(pyridin-2-yl)methylamine (0.5 g, 2.7 mmol) was added dropwise, the mixture was stirred for 30 min, and then formaldehyde (0.5 mL, 6 mmol, 37% in water) was added. After being stirred for 24 h at room temperature, the mixture was concentrated to dryness. Subsequent recrystallizations from ethanol and acetonitrile gave crystalline L^3; yield 0.66 g (1.1 mmol, 41%). Optical rotation (*S*): $[\alpha]_D^{20}$ = 18.0 (c = 1 in $CHCl_3$). $C_{34}H_{33}N_5O_5$ (591.25): calcd. C 69.02, H 5.62, N 11.84; found C 68.79, H 5.57, N 11.70. FAB-MS: calcd. for [L^3 + H]$^+$ 591.7; found 592.3. ^1H NMR (400 MHz, $CDCl_3$): δ = 1.97 (s, 1 H, N-CH_3), 3.22 (d, ^2J = 11.9 Hz, 2 H, CH_{ax}-CH_{eq}), 3.35 (d, ^2J = 11.9 Hz, 2 H, CH_{ax}-CH_{eq}), 3.73 (s, 3 H,

Table 3. Details of the crystal structure determinations.

	L^2	L^3	$[Fe(R\text{-}L^2)(Cl)]^+$	$[Fe(L^3)(Cl)]^+$
Formula	$C_{41}H_{37}N_{11}O_{19}$	$C_{34}H_{33}N_5O_5$	$C_{31}H_{38}Cl_2FeN_6O_7$	$C_{38}H_{49}Cl_2FeN_5O_9$
Crystal system	triclinic	monoclinic	orthorhombic	monoclinic
Space group	$P\bar{1}$	$C2/c$	$P2_12_12_1$	$P2_1/n$
a [Å]	11.1585(11)	29.2866(14)	9.6726(12)	13.768(2)
b [Å]	12.8329(12)	10.1952(5)	14.6784(18)	15.390(2)
c [Å]	16.9293(16)	20.8746(10)	23.256(3)	19.023(3)
α [°]	103.290(2)			
β [°]	106.284(2)	105.716(1)		102.374(3)
γ [°]	101.099(2)			
V [Å^3]	2177.3(4)	5999.8(5)	3301.8(7)	3938(1)
Z	2	8	4	4
M_r	987.82	591.65	733.42	846.57
$F(000)$	1024	2496	1528	1776
d_c [Mg m^{-3}]	1.507	1.310	1.475	1.428
μ(Mo-K_α) [mm^{-1}]	0.122	0.090	0.675	0.580
Max., min. transmission factors	0.8623, 0.8166	0.7464, 0.6954	0.7464, 0.6933	0.7464, 0.6803
θ range [°]	1.8 to 32.2	2.0 to 30.5	2.2 to 30.5	2.0 to 27.9
Index ranges (indep. set)	$-16 \le h \le 15$, $-18 \le k \le 18$, $0 \le l \le 24$	$-41 \le h \le 40$, $0 \le k \le 14$, $0 \le l \le 29$	$-13 \le h \le 13$, $0 \le k \le 20$, $0 \le l \le 33$	$-18 \le h \le 17$, $0 \le k \le 20$, $0 \le l \le 25$
Reflections measured	54739	146774	80399	81221
Unique [R_{int}]	14273 [0.0390]	9164 [0.0530]	10071 [0.0920]	9382 [0.0833]
Observed [$I \ge 2\sigma(I)$]	10591	6797	7859	6113
Parameters refined	732	475	434	478
GooF on F^2	1.027	1.087	1.059	1.047
R indices [$F \ge 4\sigma(F)$] $R(F)$, $wR(F^2)$	0.0500, 0.1215	0.0536, 0.1469	0.0404, 0.0748	0.0444, 0.1023
R indices (all data) $R(F)$, $wR(F^2)$	0.0752, 0.1372	0.0723, 0.1576	0.0701, 0.0858	0.0928, 0.1220
Absolute structure parameter			–0.006(12)	
Largest residual peaks [e Å^{-3}]	0.564, –0.591	0.530, –0.274	0.415, –0.380	0.783, –0.464

O-CH_3), 3.76 (s, 3 H, O-CH_3), 4.50 (d, ^3J = 9.1 Hz, 2 H, N-C*H*), 4.58 (s, 1 H, Py-C*H*-Ph), 7.05–8.55 (m, 17 H, H_{Ar}) ppm. ^{13}C NMR (50 MHz, $CDCl_3$): δ = 41.84 (N-*C*H_3), 52.19/52.25 (2 C, O-*C*H_3), 55.56 (2 C, N-*C*H_2), 56.39 (2 C, N-*C*H-Py), 63.14/63.25 (2 C, O-*C*H_3), 74.31 (Py-CH-Ph), 122.06, 122.69, 122.78, 124.35, 124.83, 127.43, 128.13, 128.89, 136.07, 136.09, 136.33, 140.03, 148.78, 149.19, 149.22, 157.46, 157.49, 161.12 (C_{Ar}); 168.89/168.91 (2 C, *C*OOCH$_3$), 202.14 (*C*=O) ppm.

[Fe(L^2)(OTf)](OTf): Under anaerobic conditions, (*R*)-L^2 (1.0 g, 1.9 mmol) and $[Fe(MeCN)_2](OTf)_2$ (OTf = $CF_3SO_3^-$) (0.82 g, 1.9 mmol) were dissolved in anhydrous acetonitrile (15 mL), and the resulting solution was stirred for 12 h at room temperature. After reducing the volume to 5 mL in vacuo, anhydrous ether (10 mL) was added, and the formed precipitate was filtered off. Subsequent recrystallization with acetonitrile/ether yielded the pure complex as a yellow solid; yield 1.2 g (1.4 mmol, 73%). Optical rotation (*S*): $[\alpha]_{20}^{632.5}$ = 41.0 (*c* = 0.5, in MeCN); (*R*): $[\alpha]_{20}^{632.5}$ = –40.0 (*c* = 0.5, in MeCN). $C_{31}H_{31}F_6FeN_5O_{11}S_2$ (883.07): calcd. C 42.14, H 3.54, N 7.93; found C 42.03, H 3.66, N 7.93. $C_{31}H_{33}F_6FeN_5O_{12}S_2$ {[Fe(L^2)(OTf)](OTf)·H_2O} (901.08): calcd. C 41.30, H 3.69, N 7.77; found C 42.03, H 3.66, N 7.77. FAB-MS: calcd. for [L^{2}Fe-OTf]$^+$ 734.5; found 734.3. This was the complex used for electrochemistry, spectroscopy, and catalysis; in not entirely water-free solutions, this is the hydrate (hydrolysis of the keto group at C9 of the bispidine backbone).[8] Crystals of the chlorido complex (starting with $FeCl_2$) were obtained for X-ray analysis.

[Fe(L^3)(OTf)](OTf)·3H$_2$O: Under anaerobic conditions (*S*)-L^3 (100 mg, 0.17 mmol) and $[Fe(MeCN)_2](OTf)_2$ (74 mg, 0.17 mmol) were dissolved in anhydrous acetonitrile (5 mL), and the resulting solution was stirred for 12 h at room temperature. After reducing the volume to 1 mL in vacuo, anhydrous ether (5 m) was added, and the formed precipitate was filtered off. Subsequent recrystallization with acetonitrile/ether yielded the pure complex as yellow solid; yield 53 mg (0.06 mmol, 33%). (*S*): $[\alpha]_{20}^{632.5}$ = +21.8 (*c* = 1, in MeCN). $C_{36}H_{39}F_6FeN_5O_{14}S_2$ (999.12): calcd. C 43.25, H 3.93, N 7.01; found C 43.24, H 4.06, N 6.95. FAB-MS: calcd. for [L^{3}Fe-OTf]$^+$ (796.6); found 796.3. This was the complex used for electrochemistry, spectroscopy, and catalysis; in not entirely water-free solutions, this is the hydrate (hydrolysis of the keto group at C9 of the bispidine backbone, i.e. one of the H_2O molecules is the hydrate, one is a coligand, and the third is a water of crystallization).[8] Crystals of the chlorido complex (starting with $FeCl_2$) were obtained for X-ray analysis.

Catalytic Reactions: General conditions for the epoxidation of styrene and cyclooctene are given here for the reaction with PhIO as oxidant. Freshly prepared PhIO (46 mg, 210 μmol) was added at once to a solution of the substrate (2100 μmol) and the catalyst (2.1 μmol) in MeCN or *t*BuCH$_2$OH at 25 °C. After stirring for 24 h, the internal standard naphthalene was added. All product mixtures were filtered through a short silica plug to remove the catalyst before GC analysis with a Varian 3900 instrument, equipped with a ZB-1701 column. Quantification was done with respect to the internal standard naphthalene. The enantiomeric excess was determined by HPLC with a Hewlett–Packard HP 1090 or HP 1100 instrument equipped with a Daicel Chiracel OD-H (250 X 4.6 mm, 5 μm) with guard cartridge (10 × 4 mm, 5 μm).

Acknowledgments

Generous financial support by the Deutsche Forschungsgemeinschaft (DFG) is gratefully acknowledged.

[1] K. A. Jorgensen, *Chem. Rev.* **1989**, *89*, 431.
[2] B. C. Lane, K. Burgess, *J. Am. Chem. Soc.* **2001**, *123*, 2933.
[3] J. W. De Boer, J. Brinksma, W. R. Browne, A. Meetsma, P. L. Alster, R. Hage, B. L. Ferringa, *J. Am. Chem. Soc.* **2005**, *127*, 7990.
[4] R. Hage, J. E. Iburg, J. Kerschner, J. H. Koek, E. L. M. Lempers, R. J. Martens, U. S. Racheria, S. W. Russell, T. Swarthoff, M. R. P. van Vliet, J. B. Warnaar, L. van der Wolf, B. Krijnen, *Nature* **1994**, *369*, 637.
[5] W. Nam, *Acc. Chem. Res.* **2007**, *40*, 465.
[6] M. Costas, M. P. Mehn, M. P. Jensen, L. Que Jr., *Chem. Rev.* **2004**, *104*, 939.
[7] M. S. Chen, M. C. White, *Science* **2007**, *318*, 713.
[8] P. Comba, M. Kerscher, W. Schiek, *Prog. Inorg. Chem.* **2007**, *55*, 613.
[9] H. Börzel, P. Comba, C. Katsichtis, W. Kiefer, A. Lienke, V. Nagel, H. Pritzkow, *Chem. Eur. J.* **1999**, *5*, 1716.
[10] H. Börzel, P. Comba, H. Pritzkow, *Chem. Commun.* **2001**, 97.
[11] H. Börzel, P. Comba, K. S. Hagen, M. Kerscher, H. Pritzkow, M. Schatz, S. Schindler, O. Walter, *Inorg. Chem.* **2002**, *41*, 5440.
[12] K. Born, P. Comba, A. Daubinet, A. Fuchs, H. Wadepohl, *J. Biol. Inorg. Chem.* **2007**, *12*, 36.
[13] P. Comba, S. Kuwata, M. Tarnai, H. Wadepohl, *Chem. Commun.* **2006**, 2074.
[14] P. Comba, S. Kuwata, G. Linti, M. Tarnai, H. Wadepohl, *Eur. J. Inorg. Chem.* **2007**, 657.
[15] J. Benet-Buchholz, P. Comba, A. Llobet, S. Roeser, P. Vadivelu, H. Wadepohl, S. Wiesner, *Dalton Trans.* **2009**, 5910.
[16] J. Benet-Buchholz, P. Comba, A. Llobet, S. Roeser, P. Vadivelu, S. Wiesner, *Dalton Trans.* **2010**, *39*, 3315.
[17] M. R. Bukowski, P. Comba, A. Lienke, C. Limberg, C. Lopez de Laorden, R. Mas-Balleste, M. Merz, L. Que Jr., *Angew. Chem. Int. Ed.* **2006**, *45*, 3446.
[18] J. Bautz, M. Bukowski, M. Kerscher, A. Stubna, P. Comba, A. Lienke, E. Münck, L. Que Jr., *Angew. Chem. Int. Ed.* **2006**, *45*, 5681.
[19] J. Bautz, P. Comba, C. Lopez de Laorden, M. Menzel, G. Rajaraman, *Angew. Chem. Int. Ed.* **2007**, *46*, 8067.
[20] P. Comba, M. Maurer, P. Vadivelu, *J. Phys. Chem. A* **2008**, *112*, 13028.
[21] P. Comba, M. Maurer, P. Vadivelu, *Inorg. Chem.* **2009**, *48*, 10389.
[22] P. Comba, S. Fukuzumi, H. Kotani, S. Wunderlich, *Angew. Chem. Int. Ed.* **2010**, *49*, 2622.
[23] D. Wang, K. Ray, E. R. Farkuhar, J. R. Frisch, L. Gomez, T. A. Jackson, M. Kerscher, A. Waleska, P. Comba, M. Costas, L. Que Jr., unpublished results.
[24] P. Comba, A. Lienke, *Inorg. Chem.* **2001**, *40*, 5206.
[25] P. Comba, M. Kerscher, M. Merz, V. Müller, H. Pritzkow, R. Remenyi, W. Schiek, Y. Xiong, *Chem. Eur. J.* **2002**, *8*, 5750.
[26] P. Comba, W. Schiek, *Coord. Chem. Rev.* **2003**, *238–239*, 21.
[27] C. Bleiholder, H. Börzel, P. Comba, R. Ferrari, A. Heydt, M. Kerscher, S. Kuwata, G. Laurenczy, G. A. Lawrance, A. Lienke, B. Martin, M. Merz, B. Nuber, H. Pritzkow, *Inorg. Chem.* **2005**, *44*, 8145.
[28] A. Anastasi, P. Comba, J. McGrady, A. Lienke, H. Rohwer, *Inorg. Chem.* **2007**, *46*, 6420.
[29] P. Comba, M. Merz, H. Pritzkow, *Eur. J. Inorg. Chem.* **2003**, 1711.
[30] H. Brummer, M. Niemetz, *Monatsh. Chem.* **2002**, *133*, 115.
[31] G. Alvaro, G. Martelli, D. Savoia, *J. Chem. Soc. Perkin Trans. 1* **1998**, 775.
[32] J. W. Canary, S. A. Craig, J. M. Castagnetto, Y. H. Chiu, P. J. Toscano, Y. Wang, *Inorg. Chem.* **1998**, *37*, 6255.
[33] H. Börzel, P. Comba, K. S. Hagen, M. Merz, Y. D. Lampeka, A. Lienke, G. Linti, H. Pritzkow, L. V. Tsymbal, *Inorg. Chim. Acta* **2002**, *337*, 407.
[34] A. G. Orpen, L. Brammer, F. H. Allen, O. Kennard, D. G. Watson, R. Taylor, *J. Chem. Soc., Dalton Trans.* **1989**, 1.
[35] C. V. Sastri, K. Oh, Y. J. Lee, M. S. Seo, W. Shin, W. Nam, *Angew. Chem. Int. Ed.* **2006**, *45*, 3992.
[36] M. J. Collins, K. Ray, L. Que Jr., *Inorg. Chem.* **2006**, *45*, 8009.
[37] L. D. Slep, A. Mijovilich, W. Meyer-Klaucke, T. Weyhermüller, E. Bill, E. Boothe, F. Neese, K. Wieghardt, *J. Am. Chem. Soc.* **2003**, *125*, 15554.
[38] Y.-M. Lee, H. Kotani, T. Suenobu, W. Nam, S. Fukuzumi, *J. Am. Chem. Soc.* **2008**, *130*, 434.
[39] D. Wang, M. Zhang, P. Bühlmann, L. Que Jr., *J. Am. Chem. Soc.* **2010**, *132*, 7638–7644.
[40] P. Comba, A. F. Sickmüller, *Inorg. Chem.* **1997**, *36*, 4500.
[41] There is an obvious relation between the driving force and the efficiency (kinetics), and the correlation between yield (TON) and driving force is most likely related to the suppression of slower side reactions. We are therefore currently also studying various possible pathways for the deactivation of the catalysts.
[42] A. Anastasi, A. Lienke, P. Comba, H. Rohwer, J. E. McGrady, *Eur. J. Inorg. Chem.* **2007**, 65.
[43] Note that for styrene there is also an increase of the epoxide vs. aldehyde selectivity with an increasing redox potential, but this might be fortuitous, and a correlation based on only three catalysts is a dangerous interpretation in general.
[44] *SAINT*, Bruker AXS, **1997**–2008.
[45] R. H. Blessing, *Acta Crystallogr., Sect. A* **1995**, *51*, 33.
[46] G. M. Sheldrick, *SADABS*, Bruker AXS, **2004**–**2008**.
[47] G. M. Sheldrick, *SHELXS-97*, University of Göttingen, Göttingen, **1997**.
[48] G. M. Sheldrick, *Acta Crystallogr., Sect. A* **2008**, *64*, 112.
[49] P. T. Beurskens in *Crystallographic Computing 3*, (Eds.: G. M. Sheldrick, C. Krüger, R. Goddard), Clarendon Press, Oxford, UK, **1985**, p. 216; P. T. Beurskens, G. Beurskens, R. de Gelder, J. M. M. Smits, S. Garcia-Granda, R. O. Gould, *DIRDIF 2008*, Raboud University Nijmegen, The Netherlands, **2008**.
[50] M. C. Burla, R. Caliandro, M. Camalli, B. Carrozzini, G. L. Cascarano, L. De Caro, C. Giacovazzo, G. Poidori, R. Spagna, *J. Appl. Crystallogr.* **2005**, *38*, *381*; M. C. Burla, R. Caliandro, M. Camalli, B. Carrozzini, G. L. Cascarano, L. De Caro, C. Giacovazzo, G. Polidori, R. Spagna, *SIR2004*, CNR IC, Bari, Italy, **2004**.
[51] G. M. Sheldrick, *SHELXL-97*, University of Göttingen, Göttingen, **1997**.
[52] P. van der Sluis, A. L. Spek, *Acta Crystallogr., Sect. A* **1990**, *46*, 194.
[53] A. L. Spek, *J. Appl. Crystallogr.* **2003**, *36*, 7; A. L. Spek, *PLATON*, Utrecht University, The Netherlands.

Received: March 1, 2011
Published Online: April 20, 2011

